Experimental validation of a time domain simulation of high frequency ultrasonic propagation in a suspension of rigid particles

Belfor Galaz
Laboratoire d'Imagerie Paramétrique, UPMC Univ Paris 6, and CNRS, LIP, UMR 7623, 15 rue de l'École de Médecine, 75006 Paris, France; and Department of Physics, Universidad de Santiago de Chile (USACH), Ecuador 3493, Santiago, Chile

Guillaume Haïat[a)]
CNRS, Laboratoire de Recherches Orthopédiques, Université Paris 7, UMR CNRS 7052 B2OA, 10 Avenue de Verdun, 75010 Paris, France

Romain Berti and Nicolas Taulier
Laboratoire d'Imagerie Paramétrique, UPMC Paris 6, and CNRS, LIP, UMR 7623, 15 rue de l'École de Médecine, 75006 Paris, France

Jean-Jacques Amman
Department of Physics, Universidad de Santiago de Chile (USACH), Ecuador 3493, Santiago, Chile

Wladimir Urbach
Laboratoire d'Imagerie Paramétrique, UPMC Paris 6, and CNRS, LIP, UMR 7623, 15 rue de l'École de Médecine, 75006 Paris, France; and Laboratoire de Physique Statistique de l'École Normale Supérieure de Paris, CNRS UMR 8550, 24 rue Lhomond, 75005 Paris, France

Ultrasonic propagation in suspensions of particles is a difficult problem due to the random spatial distribution of the particles. Two-dimensional finite-difference time domain simulations of ultrasonic propagation in suspensions of polystyrene 5.3 μm diameter microdisks are performed at about 50 MHz. The numerical results are compared with the Faran model, considering an isolated microdisk, leading to a maximum difference of 15% between the scattering cross-section values obtained analytically and numerically. Experiments are performed with suspensions in through transmission and backscattering modes. The attenuation coefficient at 50 MHz (α), the ultrasonic velocity (V), and the relative backscattered intensity (I_B) are measured for concentrations from 2 to 25 mg/ml, obtained by modifying the number of particles. Each experimental ultrasonic parameter is compared to numerical results obtained by averaging the results derived from 15 spatial distributions of microdisks. α increases with the concentration from 1 to 17 dB/cm. I_B increases with concentration from 2 to 16 dB. The variation of V versus concentration is compared with the numerical results, as well as with an effective medium model. A good agreement is found between experimental and numerical results (the larger discrepancy is found for α with a difference lower than 2.1 dB/cm). © *2010 Acoustical Society of America.* [DOI: 10.1121/1.3270399]

I. INTRODUCTION

The propagation of acoustic waves through particles dispersed in a fluid (suspension) is relevant to many applications, including the ultrasonic characterization of biological tissues such as blood (Haider *et al.*, 2000) or ultrasound contrast agents (Bleeker *et al.*, 1990) of emulsion (McClements, 1992), and to the acoustic propagation in underwater acoustics (for example, sandy suspensions) (Thorne and Campbell, 1992; Thorne *et al.*, 1993; Thorne and Buckingham, 2004). In addition, suspensions of elastic spheres have been proposed as acoustic calibration standards (Rhyne *et al.*, 1986).

However, predicting the acoustic wave behavior of such systems remains difficult, due to possible multiple scattering phenomena between particles, mode conversion, and apparent disorder of the particles' spatial distribution. The propagation of sound waves through suspensions of different natures has been the subject of many studies since the pioneer work of Tindall (1875), Rayleigh (1872), and Sewell (1910). A comprehensive review of wave propagation in suspensions has been written by Temkin (2001).

Briefly, suspensions have been treated by some authors as a two-phase fluid (Temkin and Dobbins, 1966; Harker and Temple, 1988; Atkinson and Kytomaa, 1992), while others (Hovem, 1980; Ogushwitz, 1985; Gibson and Nafi Toksoz, 1989) have modeled suspensions as a porous solid whose rigidity can be varied by means of adjustable parameters,

---

a)Author to whom correspondence should be addressed. Electronic mail: guillaume.haiat@univ-paris-diderot.fr

which is a model appropriate for media where a solid skeleton exists, but seems limited for suspensions of free particles such as those treated here.

The scattering theory, also called Epstein, Carhart, Allegra, and Hawley (ECAH) theory, is based on the work of Epstein and Carhart (1953) and Allegra and Hawley (1972), which has been extended by others (Hay and Mercer, 1985; Hay and Schaafsma, 1989). The ECAH theory was originally developed, considering a superposition of each particle contribution, and therefore did not consider multiple scattering. In consequence, several different approaches have been followed to modify the ECAH theory in order to incorporate multiple scattering (see, for example, Foldy, 1945; Waterman and Truell, 1961; Berryman, 1980a, 1980b; Mobley *et al.*, 1999). The coupled phase theory (Harker and Temple, 1988; Evans and Attenborough, 1997; Baudoin *et al.*, 2007) is another but powerful approach based on the two-phase hydrodynamic equations. The main difference between the coupled phase and the scattering approaches is that coupled phase theory is self-consistent. The self-consistency is generated by the use of volume averaged field variables (Margulies and Schwartz, 1994). Finally, Temkin (1998, 2000) also developed a theoretical framework applicable to a wide frequency range to model the propagation in dilute suspensions.

Time domain numerical simulation tools have not been applied to model ultrasound propagation in such complex heterogeneous media. A potential advantage of a numerical approach is its ability to solve complex problems that may become rapidly intractable when following purely analytical approaches in the frequency domain. Another advantage of time domain numerical approaches is that it allows simulating rf signals directly in the time domain, avoiding reconstructions from the frequency domain (Insana *et al.*, 1990; Doyle, 2006). Working in the time domain is interesting because (i) it allows a better comparison with the experimental signals, which are obtained in the time domain, and (ii) ultrasonic velocities measured in the time domain using different markers (such as the first zero crossing velocity) have been shown to be adapted for velocity measurements in a dispersive media such as bone (Haiat *et al.*, 2006).

The aim of this work is to examine the problem of wave propagation at high frequency (50 MHz) in suspensions of solid particles immersed in water using two-dimensional (2D) finite-difference time domain (2D FDTD) numerical simulation tools. The main advantage of this numerical method is to deal with large populations of particles, allowing to simulate multiple scattering effects in the time domain. The originality of the present approach is to account for the spatial distribution of the particles to compute the ultrasonic response of the suspension. Specifically, the 2D FDTD simulation code is validated by comparing the results with (i) analytical results obtained from the Faran theory and (ii) experimental results obtained with a solution of latex polystyrene microspheres of 5.3 μm diameter.

II. MATERIALS AND METHODS

A. Two-dimensional numerical modeling

2D numerical simulations of ultrasonic wave propagation through randomly distributed microdisk solutions are
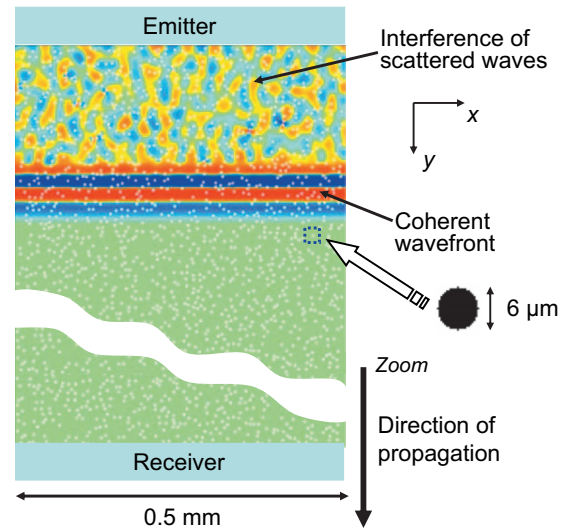

FIG. 1. Image illustrating the simulated propagation of ultrasonic wave in a suspension of disk-shaped polystyrene particles. The curved separation represents an arbitrary split of the simulation domain. In the upper part of the figure, the color codes the amplitude of the displacement as a function of position (direction y is parallel to the direction of propagation and x is perpendicular) at a given time. The coherent wavefront may be distinguished in red below the complicated wave field corresponding to interference of waves scattered by the particles. In the lower part, the figure displays the random distribution of the particles. On the right hand side, an isolated particle is shown where black pixels correspond to elastic polystyrene.

performed using SIMSONIC, a FDTD simulation software. This software has been developed by the Laboratoire d'Imagerie Paramétrique, and its description and validation can be found elsewhere (Bossy *et al.*, 2004, 2005; Haiat *et al.*, 2007). Briefly, it uses an algorithm based on the spatial and temporal discretizations of the two following coupled first-order equations describing a 2D linear elastic wave propagation (Bossy *et al.*, 2004):

$$\frac{\partial v_i}{\partial t} = \frac{1}{\rho(\vec{r})} \frac{\partial \sigma_{ij}}{\partial r_j},$$

$$\frac{\partial \sigma_{ij}}{\partial t} = C_{ijkl} \frac{\partial v_k}{\partial r_l}, \tag{1}$$

where $\vec{r}$ is the 2D position vector, $\vec{v}$ is the displacement velocity, σ is the stress tensor, and C is the stiffness tensor. The discretization is performed following the "de Virieux" (Virieux, 1986; Graves, 1996) resolution scheme with a time step, which is automatically deduced from the required stability condition described in Virieux, 1986 and Graves, 1996. The main assumptions of the model are as follows: (i) All absorption phenomena are neglected, (ii) all heat transfer phenomena are neglected, and (iii) the temperature field is assumed to be constant and homogeneous. However, the model fully takes into account all reflection and refraction effects, as well as mode conversions.

The ultrasonic propagation is simulated in a 0.5 $\times$ 1 mm^2 rectangular domain, as shown in Fig. 1. The longest length is along the y-axis, which is also the direction of the propagation. A linear ultrasound pressure source of 0.5 mm length located at $y=0$ emits a broadband pressure pulse

J. Acoust. Soc. Am., Vol. 127, No. 1, January 2010

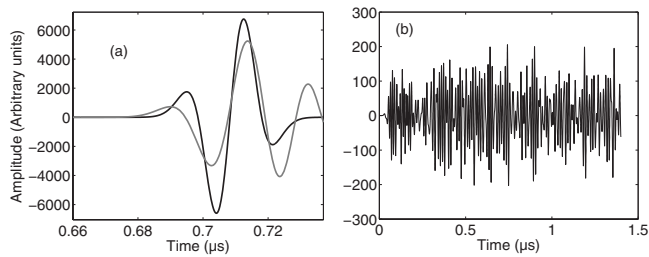Galaz *et al.*: Time domain simulation in polystyrene suspension   149

FIG. 2. Typical simulated rf signals: (a) The signal in water (in black) is identical in shape to the signal generated by the emitter. In gray: the rf signal transmitted in suspension made of 5.3 μm disk-shaped polystyrene particles immersed in water. The particle concentration is $C=13.4$ mg/ml. The value of the velocity (respectively, attenuation coefficient at 50 MHz) is equal to 1505 m/s (respectively, 4.46 dB/cm). (b) Backscattered rf signal obtained with the same suspension. The corresponding value of the relative backscattering intensity is equal to 10.6 dB.

shown in black in Fig. 2(a), with a center frequency equal to 50 MHz (bandwidth 35–62 MHz at -3 dB). To ensure plane wave propagation, symmetric boundary conditions are applied to the box sides located at $x=0$ and 0.5 mm, parallel to the y-axis. In order to avoid unphysical reflections due to the boundaries of the simulation mesh, perfectly matched layers (Collino and Tsogka, 2001) are positioned at $y=0$ and 1 mm.

Two linear receivers located at $y=0$ and 1 mm provide both backscattered and transmitted signals through a spatial average of the displacement over the entire transducer width (i.e., 0.5 mm). The chosen pixel size is equal to 0.25 μm, which is a compromise between an acceptable spatial resolution and a reasonable computational time.

Similarly to what was done previously (Bossy *et al.*, 2005; Haiat *et al.*, 2007, 2008), the numerical simulation was performed considering a plane wave propagation because this situation mimics what happens at the focus of a transducer such as the one used in the experiments.

An iterative probabilistic procedure was used to randomly insert N identical disk-shaped particles in the two-dimensional blank domain. During this procedure, the insertion of a particle is accepted only if the surface area of the particle is entirely included within the domain and if the particle surface area does not intercept the surface area of another previously inserted particle. If these conditions are not fulfilled, another location is randomly selected. This process is iterated until N particles are finally inserted in the domain.

We use this procedure to insert homogeneous polystyrene microparticles of 5.3 μm diameter. To define the region of the grid corresponding to such a homogeneous disk of radius R, having its center located at (x_0, y_0), all pixels having their center at a distance lower than R were identified and their material property was assigned to that of polystyrene. The right part of Fig. 1 shows the inserted disk-shaped particle obtained by this procedure, where the black pixels correspond to polystyrene. Figure 1 also shows an image corresponding to the ultrasonic propagation in this heterogeneous medium where the color codes the amplitude of the displacement as a function of space.

FDTD simulations require as input parameters mass densities and stiffness coefficients of all materials used in the simulation. One major difficulty is to find the most accurate parameters since they will influence the quality of the simulation predictions. We could not measure the transverse and longitudinal wave speeds in our polystyrene spheres; therefore, we started our simulations with values for polystyrene found in literature (Adjadj *et al.*, 2003; Wear, 2005). Then, we considered a variation of the longitudinal velocity in polystyrene ($V_{L,\text{PS}}$) in order to better fit our experimental data. Best agreement was achieved for a value of $V_{L,\text{PS}}$ 20%, lower than the value found in the literature. In consequence, all simulations were performed with $V_{L,\text{PS}}=2000$ m/s and $V_{T,\text{PS}}=1155$ m/s, the value of $V_{T,\text{PS}}$ corresponding to Poisson's ratio equal to 0.25.

B. Experimental measurements

Measurements were performed in solutions of microspheres of 5.3 μm diameter, made of latex polystyrene (Corpuscular Inc., Cold Spring, NY). The solution was stabilized at 25.0 ± 0.1 °C using an external control temperature system. The ultrasonic pulses were generated by transducers coupled with a 33250A Agilent pulse generator (Santa Clara, CA). The emitted and received signals were digitalized at a frequency of 200 MHz by a Lecroy oscilloscope (Chestnut Ridge, NY).

Backscattering measurements were performed using a 3 mm deep cylindrical aluminum cell filled with 1.5 ml of microsphere solution. The exposure chamber has an internal diameter of 2.5 cm. A polyvinyl chloride (PVC) film is placed on top of the solution to hermitically separate it from water added on top of the film. Agitation was maintained inside the solution; thanks to a small off-centered stirring bar. A 50 MHz polyvinylidene fluoride broadband Panametrics (model PI57-1) transducer (15.8 mm focal length and a lateral resolution of 0.9 mm at the focal point) was immersed in water and focused using an acoustic lens in the polystyrene solution at approximately 1 mm below the PVC film to avoid any contribution coming from the film. A series of sinusoidal pulses of 0.2 μs was sent by the amplifier to the transducer every 10 ms, leading to a broadband ultrasonic pulse of center frequency of 50 MHz, generated in the solution. Signals diffused by microspheres in solution were collected by the same transducer.

To measure attenuation and ultrasonic velocity, classical transmission measurements were performed using planar transducers similar to those previously described for the receiver and emitter, except that no acoustical lenses were used. A time marker (the time of the first zero crossing) was used for the reference signal and the signal transmitted through the suspension in order to derive the ultrasonic velocity. This time of flight method is described in more detail in Haiat *et al.*, 2005, 2006. The emitter and receiver were coaxially aligned and operated in transmission. They were immersed in the microsphere solution and separated by a distance of 6.5 mm. Each rf signal was estimated by performing an average of over 100 signals in order to reduce the effect of noise. Knowing the distance between the two transducers from preliminary measurements (using distilled water, which has a known sound velocity), the speed of sound was estimated with a reproducibility better than 0.1 m/s.

C. Comparison between numerical approach and experiments

In order to compare 2D simulations with three-dimensional (3D) experiments, a 2D concentration equivalent to the experimental one needed to be determined. We chose a method based on the mean distance between a particle and its closest neighbor since it is a meaningful parameter in two and three dimensions. For N randomly distributed particles within a sufficiently large 2D domain of surface area S, the mean distance D_2 between the center of one particle and the center of its closest neighbor is given by

$$D_2 = \sqrt{\frac{S}{N}}. \tag{2}$$

In the case of a 3D distribution, the inter-particle distance is given by

$$D_3 = \sqrt[3]{\frac{M}{C}}, \tag{3}$$

where M is the mass of a particle and C is the particle concentration in the solution (in mg/ml). The assumption used herein is that the distance between two particles must be the same in two and three dimensions; i.e., $D_2 = D_3$. This leads to the following relation between N and C:

$$C = M \left(\frac{N}{S}\right)^{3/2}, \tag{4}$$

which is used to relate N to the corresponding value of the concentration in three dimensions. The mass density of polystyrene was taken equal to 1.05 g/ml, which leads to a value of M equal to 8.18×10^{-11} g for a 5.3 μm diameter particle.

D. Determination of the ultrasonic parameters

Basic signal processing techniques were applied to the simulated and experimental rf signals to retrieve the ultrasound properties of the 2D domain. An example of simulated rf signal obtained in transmission and in backscattering is shown in Figs. 2(a) and 2(b), respectively. Three parameters were extracted from the simulations and experimental measurements: the speed of sound V, the attenuation coefficient $\alpha(f)$, and the apparent backscattered coefficient $ABC(f)$. Since absorption is neglected in simulations, the attenuation obtained *in silico* is only due to scattering phenomena, and the corresponding $\alpha(f)$ value, in decibel, is given by D'Astous and Foster (1986) as follows:

$$\alpha(f) = \frac{20}{L} \log\left(\frac{S_{\text{ref}}(f)}{S_{\text{sol}}(f)}\right), \tag{5}$$

where L is the path length of sound propagation. In polystyrene microparticule solutions, $L \sim 6.5$ mm and *in silico*, $L = 1$ mm. $S_{\text{ref}}(f)$ and $S_{\text{sol}}(f)$ are, respectively, the power spectrum densities (PSDs) of the signal transmitted in water and in the solution, obtained by using a fast Fourier transform. The apparent backscattered coefficient $ABC(f)$, expressed in decibel, is given by Chaffaï *et al.* (2000) as follows:
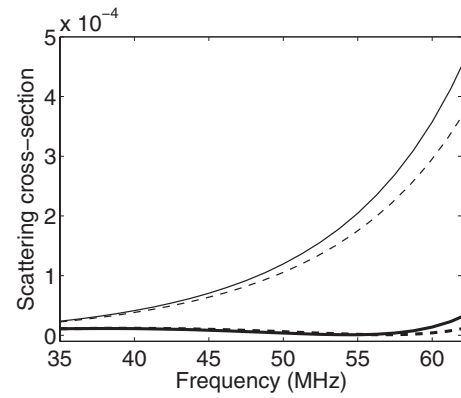

FIG. 3. Scattering cross-section obtained with the Faran model (dashed lines) and the numerical simulation (solid lines) at angles of 180° (thick lines) and 90° (thin lines) from the incident beam.

$$ABC(f) = 20 \log\left(\frac{S_b(f)}{S_{\text{ref}}(f)}\right), \tag{6}$$

where $S_b(f)$ is the PSD of the backscattered signal recorded by the transducer located at $y = 0$. The relative backscattered intensity I_B (which does not depend on the frequency) is then computed by averaging the apparent backscattered coefficient $ABC(f)$ over the frequency bandwidth of interest (35–62 MHz). The experimental precision on $\alpha(f)$ and I_B is equal, respectively, to 4 dB/cm and 1 dB.

III. RESULTS AND DISCUSSION

In order to validate our numerical approach in the framework of particle suspensions, we first carried out simulations in a 2D domain containing a single homogenous polystyrene disk with a diameter equal to 6 μm. This kind of system has been analytically solved by Faran (1951) for any angle of observation and of incidence. Figure 3 shows the comparison between the scattering cross-section (at 180° and 90°) obtained (i) with the analytical Faran model applied to a lossless isotropic elastic cylinder immersed in water and (ii) by computing the square of the amplitude ratio of the finite-difference time domain numerically simulated spectra of the scattered signal to the incident signal. The discrepancy between the analytical and simulated results, which increases up to 15% as the frequency reaches 62 MHz, is due to the (constant) spatial discretization (0.25 μm) used in the simulation code and to the fact that the scatterers are not strictly circular, as shown in Fig. 1. Decreasing the pixel size (down to 0.1 μm) leads to a decrease in the discrepancy between analytical and numerical results down to 5%. However, the choice of the value of the resolution equal to 0.25 μm corresponds to a compromise between reasonable computation time and memory requirements and an acceptable discrepancy between analytical and numerical results.

Our investigation was extended to the case of a distribution of similar homogenous polymer disks. For this case, to the best of our knowledge, there is no analytical model available in the time domain, so we confronted our simulation results with experimental values measured on solutions of polystyrene microspheres of the same diameter.

J. Acoust. Soc. Am., Vol. 127, No. 1, January 2010

Galaz *et al.*: Time domain simulation in polystyrene suspension   151

TABLE I. Number N of particles accounted for in the simulation domain and the corresponding concentration.

N	250	500	1000	1500	2000	2500
C (mg/ml)	0.92	2.59	7.3	13.4	20.7	28.9

The ultrasonic properties (ultrasonic velocity, attenuation, and relative backscattered intensity) of a given solution constructed using the procedure described in Sec. II A strongly depend on the random distribution of particles, which means that the ultrasonic parameters may differ for two different solutions constructed using the same parameters. For each concentration, 15 different solutions corresponding to 15 cases with a different random placement of particles were considered and the ultrasonic parameters were averaged over the 15 solutions. This value (15) corresponds to a compromise between a reasonable computation time and an acceptable convergence of the ultrasonic parameters. An increase in the number of simulated solutions from 15 up to 25 induces a relative change in the averaged attenuation coefficient equal to 9% of the averaged signal to noise ratio of 3% and no change in the averaged velocity. All these three values are significantly lower than the standard deviation of the results, which corresponds to the variation, due to the random spatial distribution of the particles in the simulation domain.

We have investigated the effect of concentration on the speed of sound, attenuation, and backscattered intensity. Eight concentrations, ranging from 0.9 to 28.9 mg/ml, were used herein and are listed in Table I, with the corresponding values of N obtained from Eq. (4).

Ultrasonic attenuation results from a combination of scattering and absorption phenomena. The complete characterization of absorption requires the knowledge of a large number of thermophysical parameters that are, in practice, hard to quantify. That is why we do not account for absorption in the simulation. Even so, a good agreement is obtained in Fig. 4(a) between simulated and measured values of the attenuation coefficient at 50 MHz, as the averaged difference between experimental and numerical results is equal to 2.1 dB/cm.

In the experiments, the relative backscattered intensity is normalized by the electronic noise level, which is not possible in the simulations where no noise is present. Therefore, a modified backscattered intensity was defined in the simulation. We added 38.5 dB to the simulated relative backscattered intensity, so that the extrapolated value at zero concentration in microspheres falls down to zero, as shown in Fig. 4(b). Therefore, the results shown in Fig. 4(b) only compare the variation of backscattered energy versus the concentration of particles and not its absolute value.

The variation of the speed of sound (V) versus concentration is displayed in Fig. 4(c). An increase in V is obtained for both experimental and simulated values as the particle concentration increases. The velocity of the ultrasonic waves is influenced by the material properties and the density of the particles contained in the solution and to the amount of various phases present. In order to get further insight on the behavior of the velocity as a function of the concentration, an
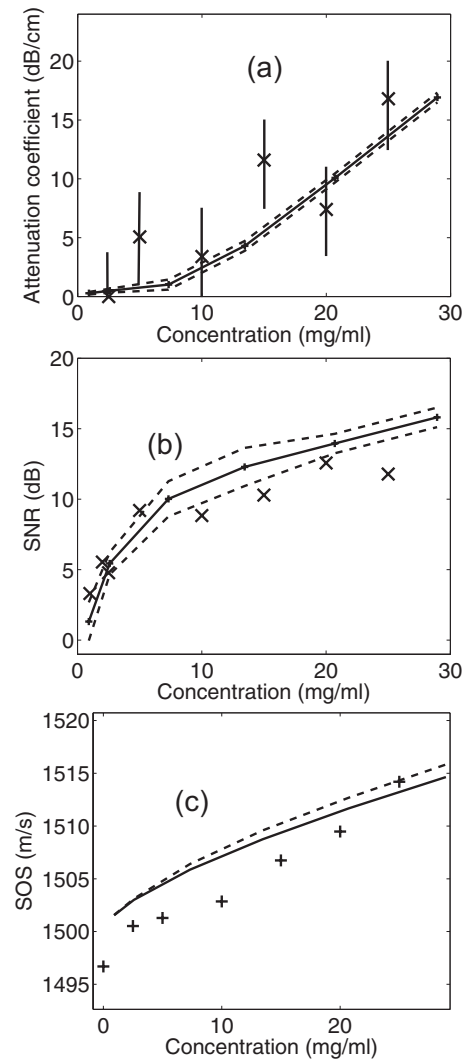

FIG. 4. (a) Mean attenuation coefficient at 50 MHz, (b) signal to noise ratio, and (c) speed of sound as a function of concentration of polystyrene microspheres. The black solid lines correspond to numerical results. The two dashed lines in (a) and (b) represent the sum and the subtraction of the mean and of the standard deviation of each quantity. The dashed line in (c) indicates the results obtained with an effective medium model (Yang and Mal, 1994). The crosses correspond to experimental results. The vertical lines in (a) indicate the experimental standard deviations. The experimental standard deviation in (b) and (c) is equal to 1 dB and 0.1 m/s, respectively.

effective medium model (Yang and Mal, 1994) was applied to the configuration of interest. This 2D model considers elastic circular scatterers immersed in an elastic matrix and takes into account multiple scattering effects. Similarly as what was done in Haïat et al., 2008 in another context, we considered a value of shear wave velocity Vs in water equal to 5 m/s. This value was chosen arbitrarily and we verified that decreasing the value of Vs down to 0.1 m/s does not modify the phase velocity, which indicates that shear wave modes propagating in the matrix do not significantly affect the phase velocity. Readers are referred to Haïat et al., 2008 for further details on the approach considered. A good agreement is obtained between the effective medium model and the numerical model, as the difference between the two results is lower than 1 m/s. This last result constitutes an additional further validation of the numerical model.

The advantage of the approach using FDTD simulations is to be able to provide a reasonable estimation of ultrasound properties of suspensions based on the chemical and physical properties of the materials. However, there are several limitations to the approach carried out in the present study. First, we use a 2D model, and 3D models would be more accurate to model the propagation in suspensions, which is possible using the SIMSONIC software (Bossy *et al.*, 2005; Haïat *et al.*, 2007). The propagation in a 2D medium of disks is different than in a 3D medium of spheres, which might explain possible discrepancies between experiments and simulations. However, the present 2D approach is a first step in studying these phenomena, and further studies are required to tackle the difficult 3D problem, which would require significantly longer time of computation and memory. Second, absorption effects are not taken into account and only the part of attenuation that depends on scattering phenomena is considered here. Third, the proposed model is simplistic because we only considered similar particles (monodisperse suspension), whereas they are, in reality, different in terms of diameter. We choose to consider monodisperse suspensions in order to study the effect of concentration independently of the diameter distribution, which corresponds to a first step in the study of such suspensions. Moreover, the precise distribution of the diameter of the polystyrene particles remains unknown and we thus did considered monodispersed suspensions. Fourth, we did not account for diffraction effects, which might modify the results obtained in backscattering since we assume a planar wave propagation in the simulation.

It should be emphasized that this work could have been carried out at any center frequency without any limitation. We choose to work around about 50 MHz because our long term goal is to provide a numerical model in order to study wave propagation through liquid filled ultrasound contrast agent used for high frequency applications such as microcirculation, ophthalmic disease diagnosis and small animal imaging, or biomicroscopy applications, which are currently investigated in the framework of our research project.

ACKNOWLEDGMENTS

Adjadj, L., Storti, G., and Morbidelli, M. (**2003**). "Ultrasound attenuation in polystyrene latexes," Langmuir **19**, 3953–3957.

Allegra, J. R., and Hawley, S. A. (**1972**). "Attenuation of sound in suspensions and emulsions: Theory and experiments," J. Acoust. Soc. Am. **51**, 1545–1564.

Atkinson, C. M., and Kytomaa, H. K. (**1992**). "Acoustic wave speed and attenuation in suspensions," Int. J. Multiphase Flow **18**, 577–592.

Baudoin, M., Thomas, J. L., Coulouvrat, F., and Lhuillier, D. (**2007**). "An extended coupled phase theory for the sound propagation in polydisperse concentrated suspensions of rigid particles," J. Acoust. Soc. Am. **121**, 3386–3397.

Berryman, J. (**1980a**). "Long-wavelength propagation in composite elastic media I. Spherical inclusions," J. Acoust. Soc. Am. **68**, 1809–1819.

Berryman, J. (**1980b**). "Long-wavelength propagation in composite elastic media II. Ellipsoidal inclusions," J. Acoust. Soc. Am. **68**, 1820–1831.

Bleeker, H. J., Shung, K. K., and Barnhart, J. L. (**1990**). "Ultrasonic characterization of AlbunexR, a new contrast agent," J. Acoust. Soc. Am. **87**, 1792.

Bossy, E., Padilla, F., Peyrin, F., and Laugier, P. (**2005**). "Three-dimensional simulation of ultrasound propagation through trabecular bone structures measured by synchrotron microtomography," Phys. Med. Biol. **50**, 5545–5556.

Bossy, E., Talmant, M., and Laugier, P. (**2004**). "Three-dimensional simulations of ultrasonic axial transmission velocity measurement on cortical bone models," J. Acoust. Soc. Am. **115**, 2314–2324.

Chaffaï, S., Roberjot, V., Peyrin, F., Berger, G., and Laugier, P. (**2000**). "Frequency dependence of ultrasonic backscattering in cancellous bone: Autocorrelation model and experimental results," J. Acoust. Soc. Am. **108**, 2403–2411.

Collino, F., and Tsogka, C. (**2001**). "Application of the PML absorbing layer model to the linear elastodynamic problem in anisotropic heterogeneous media," Geophysics **66**, 294–307.

D'Astous, F. T., and Foster, F. S. (**1986**). "Frequency dependence of ultrasound attenuation and backscatter in breast tissue," Ultrasound Med. Biol. **12**, 795–808.

Doyle, T. E. (**2006**). "Iterative simulation of elastic wave scattering in arbitrary dispersions of spherical particles," J. Acoust. Soc. Am. **119**, 2599–2610.

Epstein, P. S., and Carhart, R. R. (**1953**). "The absorption of sound in suspensions and emulsions. I. Waterfog in air," J. Acoust. Soc. Am. **25**, 553–565.

Evans, J. M., and Attenborough, K. (**1997**). "Coupled phase theory for sound propagation in emulsions," J. Acoust. Soc. Am. **102**, 278–282.

Faran, J. J. (**1951**). "Sound scattering by solid cylinders and spheres," J. Acoust. Soc. Am. **23**, 405–418.

Foldy, L. L. (**1945**). "The multiple scattering of waves. I. General theory of isotropic scattering by randomly distributed scatterers," Phys. Rev. **67**, 107–119.

Gibson, R. L. J., and Nafi Toksoz, M. (**1989**). "Viscous attenuation of acoustic waves in suspensions," J. Acoust. Soc. Am. **85**, 1925–1934.

Graves, R. (**1996**). "Simulating seismic wave propagation in 3D elastic media using staggered-grid finite differences," Bull. Seismol. Soc. Am. **86**, 1091–1106.

Haïat, G., Lhemery, A., Renaud, F., Padilla, F., Laugier, P., and Naili, S. (**2008**). "Velocity dispersion in trabecular bone: Influence of multiple scattering and of absorption," J. Acoust. Soc. Am. **124**, 4047–4058.

Haïat, G., Padilla, F., Barkmann, R., Dencks, S., Moser, U., Gluer, C. C., and Laugier, P. (**2005**). "Optimal prediction of bone mineral density with ultrasonic measurements in excised human femur," Calcif. Tissue Int. **77**, 186–192.

Haïat, G., Padilla, F., Cleveland, R. O., and Laugier, P. (**2006**). "Effects of frequency-dependent attenuation and velocity dispersion on in vitro ultrasound velocity measurements in intact human femur specimens," IEEE Trans. Ultrason. Ferroelectr. Freq. Control **53**, 39–51.

Haïat, G., Padilla, F., Peyrin, F., and Laugier, P. (**2007**). "Variation of ultrasonic parameters with trabecular bone properties: A three-dimensional model simulation," J. Bone Miner. Res. **12**, 12.

Haider, L., Snabre, P., and Boynard, M. (**2000**). "Rheo-acoustical study of the shear disruption of reversible aggregates. Ultrasound scattering from concentrated suspensions of red cell aggregates," J. Acoust. Soc. Am. **107**, 1715–1726.

Harker, A. H., and Temple, J. A. (**1988**). "Velocity and attenuation of ultrasound in suspensions of particles in fluids," J. Phys. D **21**, 1576–1588.

Hay, A., and Mercer, D. (**1985**). "On the theory of sound scattering and viscous absorption in aqueous suspensions at medium and short wavelengths," J. Acoust. Soc. Am. **78**, 1761.

Hay, A., and Schaafsma, A. (**1989**). "Resonance scattering in suspensions," J. Acoust. Soc. Am. **85**, 1124–1138.

Hovem, J. M. (**1980**). "Viscous attenuation of sound in suspensions and high porosity sediments," J. Acoust. Soc. Am. **67**, 1559–1563.

Insana, M. F., Wagner, R. F., Brown, D. G., and Hall, T. J. (**1990**). "Describing small-scale structure in random media using pulse-echo ultrasound," J. Acoust. Soc. Am. **87**, 179–192.

Margulies, T. S., and Schwartz, W. H. (**1994**). "A multiphase continuum theory for sound wave propagation through dilute suspensions of particles," J. Acoust. Soc. Am. **96**, 319–331.

McClements, D. J. (**1992**). "Comparison of multiple scattering theories with experimental measurements in emulsions," J. Acoust. Soc. Am. **91**, 849.

Mobley, J., Waters, K. R., Hall, C. S., Marsh, J. N., Hughes, M. S., Bran-

denburger, G. H., and Miller, J. G. (**1999**). "Measurements and predictions of the phase velocity and attenuation coefficient in suspensions of elastic microspheres," J. Acoust. Soc. Am. **106**, 652–659.

Ogushwitz, P. R. (**1985**). "Applicability of the Biot theory. II. Suspensions," J. Acoust. Soc. Am. **77**, 441–452.

Rayleigh, L. (**1872**). "Investigation of disturbance produced by a spherical obstacle on the waves of sound," Proc. London Math. Soc. **4**, 253–383.

Rhyne, T. L., Sagar, K. B., Wann, S. L., and Haasler, G. (**1986**). "The myocardial signature: Absolute backscatter, cyclical variation, frequency variation, and statistics," Ultrason. Imaging **8**, 107–120.

Sewell, C. J. T. (**1911**). "On the extinction of sound in a viscous atmosphere by small obstacles of cylindrical and spherical form," Philos. Trans. R. Soc. London **210**, 239–270.

Temkin, S. (**1998**). "Sound propagation in dilute suspensions of rigid particles," J. Acoust. Soc. Am. **103**, 838–849.

Temkin, S. (**2000**). "Attenuation and dispersion of sound in dilute suspensions of spherical particles," J. Acoust. Soc. Am. **108**, 126–146.

Temkin, S. (**2001**). *Elements of Acoustics* (American Institute of Physics, Melville, NY).

Temkin, S., and Dobbins, R. A. (**1966**). "Attenuation and dispersion of sound by particulate relaxation processes," J. Acoust. Soc. Am. **40**, 317–324.

Thorne, P., and Buckingham, M. (**2004**). "Measurements of scattering by suspensions of irregularly shaped sand particles and comparison with a single parameter modified sphere model," J. Acoust. Soc. Am. **116**, 2876–2889.

Thorne, P., and Campbell, S. C. (**1992**). "Backscattering by a suspension of spheres," J. Acoust. Soc. Am. **92**, 978–986.

Thorne, P., Manley, C., and Brimelow, J. (**1993**). "Measurements of the form function and total scattering cross section for a suspension of spheres," J. Acoust. Soc. Am. **93**, 243–248.

Tindall, J. (**1875**). *Sound* (Longmans, Green, and Co., London).

Virieux, J. (**1986**). "P-SV wave propagation in heterogeneous media: Velocity-stress finite-difference method," Geophysics **51**, 889–901.

Waterman, P. C., and Truell, R. (**1961**). "Multiple-scattering of waves," J. Math. Phys. **2**, 512–537.

Wear, K. A. (**2005**). "The dependencies of phase velocity and dispersion on trabecular thickness and spacing in trabecular bone-mimicking phantoms," J. Acoust. Soc. Am. **118**, 1186–1192.

Yang, R. B., and Mal, A. K. (**1994**). "Multiple-scattering of elastic waves in a fiber-reinforced composite," J. Mech. Phys. Solids **42**, 1945–1968.